Journal of Zhejiang University-SCIENCE C (Computers & Electronics)
ISSN 1869-1951 (Print); ISSN 1869-196X (Online)
www.zju.edu.cn/jzus; www.springerlink.com
E-mail: jzus@zju.edu.cn

Miniaturized fractal-shaped branch-line coupler for dual-band applications based on composite right/left handed transmission lines*

He-xiu XU†1, Guang-ming WANG[1], Pei-lin CHEN[2], Tian-peng LI[1]

([1]*Electromagnetic Field and Microwave Technique, Missile Institute, Air Force Engineering University, Sanyuan 713800, China*)

([2]*School of Electronics and Information Engineering, Northwestern Polytechnical University, Xi'an 710129, China*)

†E-mail: hxxu20008@yahoo.cn

Received Sept. 30, 2010; Revision accepted Jan. 13, 2011; Crosschecked July 29, 2011

Abstract: In this paper, novel dual-band (DB) branch-line couplers (BLCs) employing a composite right/left handed transmission line (CRLH TL) and fractal geometry are presented for the first time. The CRLH TL, with specified characteristic impedance and phase shift, consists of lumped elements for the left handed (LH) part and fractal-shaped microstrip lines (MLs) for the right handed (RH) part, which can be designed separately. Two designed BLCs are involved in size reduction, one using a 3/2 fractal curve of first iteration, the other constructed based on a hybrid shape of fractal and meandered lines. A miniaturized principle for CRLH TL realization is derived and an exact design method for fractal implementation is developed. For verification, an example coupler was fabricated and measured. Consistent numerical and experimental results confirmed the design concept, showing that the BLCs obtain DB behavior centered at 0.9 GHz and 1.8 GHz respectively with good in-band performance, except for slightly larger coupled insertion loss for the hybrid-shaped BLC case. In addition, the proposed fractal- and hybrid-shaped BLCs obtained a 49.7% and 64.1% size reduction respectively relative to their conventional counterparts working in the lower band. The most important contributions of this article are the demonstration of compatibility between the fractal and CRLH TL techniques and the provision of an alternative approach and a new concept for designing devices.

Key words: Fractal, Composite right/left handed transmission line (CRLH TL), Dual-band (DB), Miniaturization, Branch-line coupler (BLC)
doi:10.1631/jzus.C1000343 **Document code:** A **CLC number:** O441

1 Introduction

Hybrids, such as rat-race, branch-line, and coupled-line configurations, are a set of the most important and widely used passive circuits for microwave and millimeter-wave applications. When concentrating on a 90° hybrid, the branch-line coupler (BLC) is preferred. Demand for increased portability, reliability, and integrity of multi-standard communications has encouraged extensive research on miniaturized and dual-band (DB) BLCs. There are numerous publications on miniaturized BLCs for various applications. Ghali and Moselhy (2004) using fractal geometry achieved a significant 75.3% size reduction and Chen and Wang (2008) a 64.6% size reduction, based on a dual (Tang *et al.*, 2008) and discontinuous (Sun *et al.*, 2005) transmission line, slow-wave structure (Wang *et al.*, 2007), and a quasi-lumped elements approach (Liao and Peng, 2006). BLCs reported by Sun *et al.* (2005), Liao and Peng (2006), Wang *et al.* (2007), and Tang *et al.* (2008) obtained size reduction rates of 60%, 71%, 72%, and 63.9%, respectively. Although these BLCs

* Project supported by the National Natural Science Foundation of China (Nos. 60871027 and 60971118) and the National Basic Research Program (973) of China (No. 2009CB613306)

are quite compact, they are restricted to DB operation.

In recent years, the composite right/left handed transmission line (CRLH TL) concept and theory have been broadly applied to DB BLCs (Lin *et al.*, 2004; Zhang *et al.*, 2005; Bonache *et al.*, 2008; Chi and Itoh, 2009). Other techniques have also been proposed for this purpose, including BLCs employing tapped stubs (Zhang and Chen, 2007). The DB BLCs presented by Lin *et al.* (2004), Zhang *et al.* (2005), Bonache *et al.* (2008), and Chi and Itoh (2009) show relatively good performance, but would perform better if miniaturization had been given more consideration. In the BLC of Lin *et al.* (2004), the length of the quarter-wavelength branch is even longer than its conventional counterpart, thus occupying a large area. Fortunately, BLCs reported by Bonache *et al.* (2008) and Chi and Itoh (2009) achieved miniaturization scales of 39.2% and 10% respectively, while simultaneously incorporating DB performance. However, they are still far from adequate in terms of miniaturization. Most recently, the concept of fractal geometry combined with CRLH TL in the design of microwave integrated circuits (MICs) is being introduced (Xu *et al.*, 2010a; 2010b).

This new work presents an alternative method for dealing with the drawbacks of earlier methods (Lin *et al.*, 2004; Zhang *et al.*, 2005; Bonache *et al.*, 2008; Chi and Itoh, 2009). The principles and advantages of miniaturization lie in two aspects, which will be detailed in the next section.

2 Branch-line coupler design

A conventional BLC is a four-port network which can be implemented by integrating two pairs of 35.3 Ω (horizontal branch) and 50 Ω (vertical branch) microstrip lines (MLs). It can operate at its fundamental frequency and odd harmonics. However, in this study, our interest was focused on DB behavior and compactness. In this regard, we consider MLs and surface mount technology (SMT) chip lumped elements constituting the right handed (RH) and left handed (LH) contributions of 35.3 Ω and 50 Ω CRLH TL with required phase at two arbitrary bands, and then construct the MLs as 3/2 curves with hybrid shape configuration for the purpose of size reduction.

2.1 CRLH TL realization

The DB property of 35.3 Ω and 50 Ω CRLH TL has been successfully interpreted by its hyperbolic-linear dispersion relation (Lin *et al.*, 2004; Chi and Itoh, 2009) and hence is not discussed here. The well-known circuit model of a CRLH TL unit cell (Fig. 1) is provided for convenience of analysis.

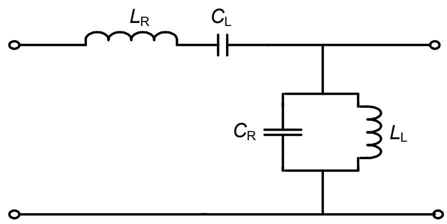

Fig. 1 Ideal circuit model of a CRLH TL unit cell

Let us begin with the fundamental theory of a balanced CRLH TL, for which the phase and characteristic impedance are given as

$$\varphi^{\mathrm{CRLH}}=\varphi^{\mathrm{LH}}+\varphi^{\mathrm{RH}}=\frac{N}{\omega\sqrt{L_{\mathrm{L}}C_{\mathrm{L}}}}-N\omega\sqrt{L_{\mathrm{R}}C_{\mathrm{R}}}, \quad (1)$$

$$Z^{\mathrm{CRLH}}=\sqrt{\frac{L_{\mathrm{R}}}{C_{\mathrm{R}}}}=\sqrt{\frac{L_{\mathrm{L}}}{C_{\mathrm{L}}}}, \quad (2)$$

where N is the number of unit cells. For the DB implementation, matching the identical terminations of impedance Z_c and phasing to φ_L, φ_H for desired operation at any pair of angular frequencies ω_L, ω_H ($\omega_L<\omega_H$) lead to

$$\varphi^{\mathrm{CRLH}}(\omega=\omega_{\mathrm{L}}=2\pi f_{\mathrm{L}})=\varphi_{\mathrm{L}}, \quad (3a)$$

$$\varphi^{\mathrm{CRLH}}(\omega=\omega_{\mathrm{H}}=2\pi f_{\mathrm{H}})=\varphi_{\mathrm{H}}, \quad (3b)$$

$$Z^{\mathrm{CRLH}}(\omega=\omega_{\mathrm{L}})=Z^{\mathrm{CRLH}}(\omega=\omega_{\mathrm{H}})=Z_{\mathrm{c}}. \quad (3c)$$

By insertion of Eqs. (1) and (2) into Eq. (3), explicit expressions for circuit parameters can be acquired for a given N after some manipulation:

$$L_{\mathrm{R}}=\frac{Z_{\mathrm{c}}[\varphi_{\mathrm{L}}(\omega_{\mathrm{L}}/\omega_{\mathrm{H}})-\varphi_{\mathrm{H}}]}{N\omega_{\mathrm{H}}[1-(\omega_{\mathrm{L}}/\omega_{\mathrm{H}})^2]}, \quad (4a)$$

$$C_{\mathrm{R}}=\frac{\varphi_{\mathrm{L}}(\omega_{\mathrm{L}}/\omega_{\mathrm{H}})-\varphi_{\mathrm{H}}}{N\omega_{\mathrm{H}}Z_{\mathrm{c}}[1-(\omega_{\mathrm{L}}/\omega_{\mathrm{H}})^2]}, \quad (4b)$$

$$L_{\mathrm{L}}=\frac{NZ_{\mathrm{c}}[1-(\omega_{\mathrm{L}}/\omega_{\mathrm{H}})^2]}{\omega_{\mathrm{L}}[\varphi_{\mathrm{L}}-\varphi_{\mathrm{H}}(\omega_{\mathrm{L}}/\omega_{\mathrm{H}})]}, \tag{4c}$$

$$C_{\mathrm{L}}=\frac{N[1-(\omega_{\mathrm{L}}/\omega_{\mathrm{H}})^2]}{\omega_{\mathrm{L}}Z_{\mathrm{c}}[\varphi_{\mathrm{L}}-\varphi_{\mathrm{H}}(\omega_{\mathrm{L}}/\omega_{\mathrm{H}})]}. \tag{4d}$$

Note that not all solutions are feasible. In certain cases, high- and low-pass cut-off frequencies may intersect the operation range for a given specification of ω_{L}, ω_{H}, φ_{L}, φ_{H}, Z_{c}, and N (Chi and Itoh, 2009). As a consequence, some solutions may fail and should be ruled out.

For DB quarter-wavelength transformer applications, there may be more than one pair of phases φ_{L}, φ_{H} meeting the request. Pairs of phases with π difference between φ_{L}, φ_{H} can be used in principle: for example, pairs of phases φ_{L}, φ_{H}=−π/2, −3π/2 (Lin *et al.*, 2004), π/2, −π/2 (Chi and Itoh, 2009), and 3π/2, π/2 would yield similar results. However, there should be a pair of phases that fulfill the aim of maximum miniaturization. As a consequence, the selection of phases φ_{L}, φ_{H} at two specified bands is important and should be carefully considered. Insertion of Eq. (1) into Eq. (3) yields

$$\varphi_{\mathrm{L}}=\frac{N}{\omega_{\mathrm{L}}\sqrt{L_{\mathrm{L}}C_{\mathrm{L}}}}-N\omega_{\mathrm{L}}\sqrt{L_{\mathrm{R}}C_{\mathrm{R}}}, \tag{5a}$$

$$\varphi_{\mathrm{H}}=\frac{N}{\omega_{\mathrm{H}}\sqrt{L_{\mathrm{L}}C_{\mathrm{L}}}}-N\omega_{\mathrm{H}}\sqrt{L_{\mathrm{R}}C_{\mathrm{R}}}. \tag{5b}$$

The coefficient K which solely determines the electrical length (namely the physical length of the ML) calculates as

$$K=N\sqrt{L_{\mathrm{R}}C_{\mathrm{R}}}=\frac{\varphi_{\mathrm{L}}\omega_{\mathrm{L}}-\varphi_{\mathrm{H}}\omega_{\mathrm{H}}}{\omega_{\mathrm{H}}^2-\omega_{\mathrm{L}}^2}. \tag{6}$$

In the study of Lin *et al.* (2004), φ_{L} and φ_{H} were set to −π/2 and −3π/2 respectively, and thus coefficient K' was obtained. The proportionality of the value K for π/2, −π/2 in this paper, to K' under angular frequencies ω_{L}, ω_{H} is determined as

$$\frac{K}{K'}=\frac{\omega_{\mathrm{H}}+\omega_{\mathrm{L}}}{3\omega_{\mathrm{H}}-\omega_{\mathrm{L}}}=\frac{\alpha+1}{3\alpha-1}<1, \tag{7}$$

with $\omega_{\mathrm{H}}=\alpha\omega_{\mathrm{L}}$ and $\alpha>1$. Eq. (7) can also be used to determine the proportionality in the 3π/2, π/2 case. The case π/2, −π/2 for φ_{L}, φ_{H} can be shown to be clearly the best choice for miniaturization. In this study, φ_{L}, φ_{H} are set to be π/2, −π/2 while f_{L}, f_{H} are designed to be 0.9 GHz and 1.8 GHz, respectively.

Since natural RH parasitics are inherent in SMT components and result in small phase delays in the LH section, they should not be ignored in practice. Nevertheless, a slight reduction of MLs can compensate for this problem. For symmetry and improved transmission properties, the TL should be terminated by two capacitors of $2C_{\mathrm{L}}$. Novel designed DB BLCs are built on a substrate with a dielectric constant (ε_{r}) of 2.65 and a thickness (h) of 0.8 mm. Detailed theoretically calculated and practical available parameters including the length l and width w of MLs are summarized in Table 1. The calculated l is slightly larger than the one used in practice which takes RH parasitics of SMT elements into account.

Table 1 Detailed physical parameters of the 35.3 Ω and 50 Ω CRLH TLs

Parameter	Value			
	35.3 Ω CRLH TL		50 Ω CRLH TL	
	Theoretical	Practical	Theoretical	Practical
L_{L} (nH)	3.97	3.9	5.63	5.6
C_{L} (pF)	3.20	3.3	2.25	2.2
$2C_{\mathrm{L}}$ (pF)	6.40	6.2	4.50	4.7
l (mm)	55.3	51	56.3	52
w (mm)	3.6	3.6	2.2	2.2

2.2 Fractal implementation

With the physical ML length (RH part) of the CRLH TL branch determined, the next step consists of constructing the MLs as fractal or meandered configurations with the same electrical performance (phase response) for further size reduction. The compaction mechanism of fractal curves and meandered lines is simple due to their space-filling properties.

The fractal geometry used in this work is a 3/2 fractal curve (Fig. 2) initially proposed for microstrip patch antenna applications (Sadat *et al.*, 2005). It has a simple generation law employing a double quadrate indentation as the generator, in which the indentation width is a quarter of the original length. The curve is determined by the Hausdorff dimension D, iteration factor (IF=1/4), and iteration order (IO). According to the rule, the fractal dimension, which can be understood as a measure of the space-filling ability of a fractal curve, is defined as

$$4\times(1/4)^{D}+4\times(1/4)^{D}=1. \tag{8}$$

Thus, D is calculated as 3/2 from Eq. (8). Because of the space-filling nature of fractal curves, the physical length of the ML can be significantly extended for a given straight dimension. The perimeter is doubled with each iteration order. Consequently, the total length after iteration level n is given by

$$L_n=2L_{n-1}=2^{n}L_0. \tag{9}$$

Consulting Eq. (9), the designed ML increases exponentially as the iteration level increases, giving the spacing-filling properties shown.

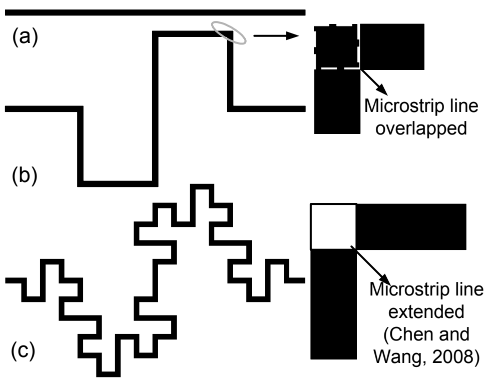

Fig. 2 The 3/2 fractal curves with zeroth (a), first (b), and second (c) iteration orders

Since many fractal segments are introduced in the fractal implementation, bends, right-angles, or chamfers are commonly used to connect these segments. Note that it is only the bend that results in the discontinuity. The non-negligible discontinuity reactance, which is the cause of transmission phase-shifting, must be properly evaluated if an exact design is required for a fractal-shaped ML with a specified phase.

The phase-shifting property, however, should be investigated by comparing the phase response of fractal-shaped MLs with different IOs (IO=0, 1, 2). To demonstrate and evaluate this effect, 50 Ω MLs with lengths and widths of 96 mm and 0.9 mm respectively, for three cases were analyzed on microwave substrate with a dielectric constant (ε_r) of 4.4 and a thickness (h) of 0.5 mm. The method of moments (MoM) based planar electromagnetic (EM) simulator Ansoft Design (version 3.5) (ANSYS Company, USA) was applied for characterization. The transmission phase response of the fractal-shaped MLs with different IOs is shown in Fig. 3a. Transmission phases shift towards lower negative values as the IO increases, which seemingly conflicts with the conclusion derived by Chen and Wang (2008) (a shift towards higher negative values). But in fact, it is the different operation at fractal right-angle bends (see Fig. 2) that gives rise to the contrary results. Lower phases for higher IOs in this paper result from neighboring segments partially overlapping, while higher phases in Chen and Wang (2008) result from MLs being partially extended. In other words, the total ML contains twice the bend length in the current work while the bend length is ruled out in Chen and Wang (2008)'s approach. Note that the bend length not only is composed of physical length but also includes a description of a compositive discontinuity effect.

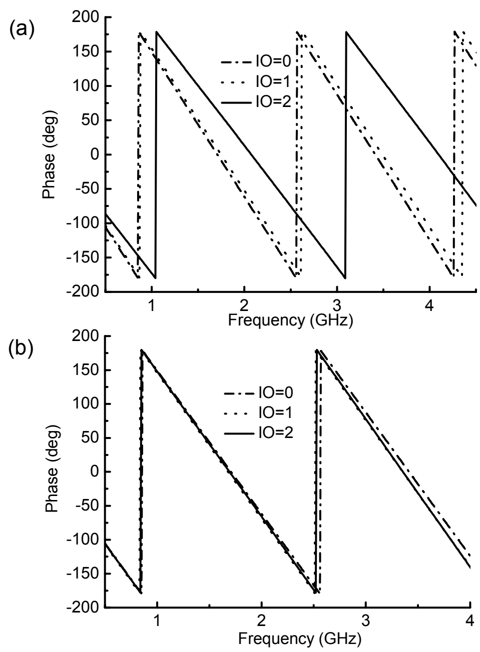

Fig. 3 Simulated transmission phase response of the fractal-shaped microstrip lines with different IOs without (a) or with (b) the exact design method

To synthesize fractal-shaped MLs for a required phase at a given frequency, a simple exact design method is derived. In this regard, the length of the conventional ML l should be extended by Δd per bend for fractal- or meander-shaped ML implementation:

$$L = l + n \cdot \Delta d, \tag{10}$$

where Δd is applied to evaluate roughly the effect of discontinuity reactance induced by each bend (Bahl, 2003).

$$\Delta d = \frac{19.2\pi h}{\sqrt{\varepsilon_{\text{eff}}} Z_{\text{c}}} \left[2 - \left(\frac{f_0 h}{0.4 Z_{\text{c}}} \right)^2 \right], \tag{11}$$

where h is the height of the substrate in mm, ε_{eff} is the effective dielectric constant, and Z_{c} is the characteristic impedance in Ω. Next, a final minor optimization of the obtained rough L is essential for an exact design. Fig. 3b shows the simulated transmission phase response of the designed MLs employing the exact design method. Almost identical phase behavior can be observed for the whole band except for a slight discrepancy for the higher band, which confirms the effectiveness of this method.

As to the second or even higher iteration for the current BLC application, segment width is constant, corresponding to the specified dielectric substrate and characteristic impedance. The segment length and the space between adjacent MLs decrease with improved iteration, which in turn degrades the BLC performance and limits its usage in practical application. However, there is insufficient space to load lumped elements in the second-order 3/2 fractal-shaped ML. Consequently, a trade-off between miniaturization and performance of BLCs should be performed. In this regard, the adoptable 3/2 fractal curve is confined to the first iteration. Despite this, we have exploited a hybrid shape of first-order 3/2 curve and a meandered line for further miniaturization of the BLC. It is evaluated in terms of its best area-filling efficiency and can be considered as a perfect substitution of a second-order 3/2 curve.

The configurations of our final BLC designs are illustrated in Fig. 4. A conventional BLC is included for comparison. The space between neighboring MLs is small due to the strong space-filling capability. The total occupied area of the novel designed BLC using a 3/2 curve is 51.8 mm×49.2 mm (including the access line), compared with 50.4 mm×36.1 mm for a hybrid-shaped BLC. Thus, fractal- and hybrid-shaped BLCs achieved size reduction of 49.7% and 64.1%, respectively, with respect to their conventional counterpart (81.3 mm×62.2 mm) operating at the lower band of 0.9 GHz. This miniaturization factor should be better (65% and 75%) if compared to CRLH TL BLCs with nonfractal geometry (about 95.3 mm×76.2 mm) as CRLH TL BLCs have identical RH electrical length (90°) with conventional pure RH BLCs and introduce additional SMT elements in the LH part for DB implementation. Thus, our proposed strategy is highly preferable for compact design.

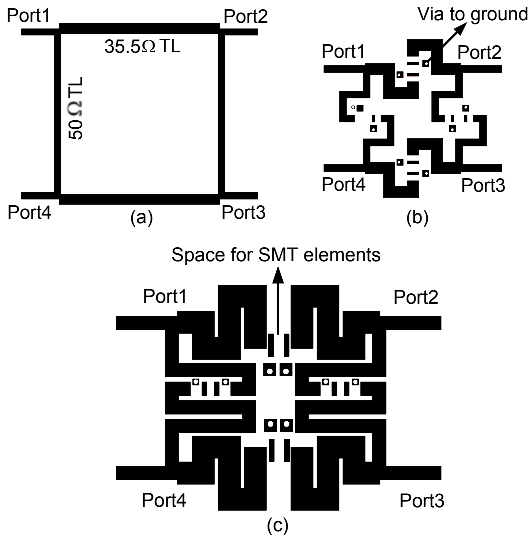

Fig. 4 Schematic of the proposed fractal-shaped BLCs
(a) Conventional design; (b) Novel design using 3/2 fractals; (c) Novel design using a hybrid shape of 3/2 fractals and meander line

3 Illustrative results

3.1 Simulated results

To illustrate the validity of the combined technology, novel designed BLCs were analyzed through dynamic links and a solver of planar EM and circuit co-simulation in MoM-based Ansoft Designer (version 3.5). The top-level circuit (composed of SMT elements) received solution data from its planar EM subcircuit (MLs). Fig. 5 shows the simulated frequency response of the proposed BLCs. DB performance is clearly apparent with a lower band at 0.9 GHz and an upper band at 1.8 GHz.

Furthermore, two most important aspects should be highlighted. First, the fractal perturbations in BLCs deteriorate the match performance to some degree; e.g., the return loss for a conventional BLC is

64 dB, compared with 28.8 dB for the lower-band and 29.8 dB for the upper-band in the case of a fractal-shaped BLC, and even worse values of 25.3 dB and 18.6 dB respectively, for the hybrid shape case. The resultant high reflection losses can be successfully explained through the generation of a mass of fractal bends during the fractal implementation. Second, the output magnitude imbalance, especially in the upper band, becomes larger as the miniaturization factor increases, essentially induced by the larger coupled insertion loss, e.g., the maximum of 3.52 dB for the fractal shape case, and 4.1 dB for the hybrid shape case. The relatively large coupled insertion loss is due mainly to the coupling between adjacent MLs within miniaturized space. Note that although the performance of the BLCs worsens to some degree, it is still within normal levels within the scope of practical application and these BLCs also have the advantage of being highly integrated circuits.

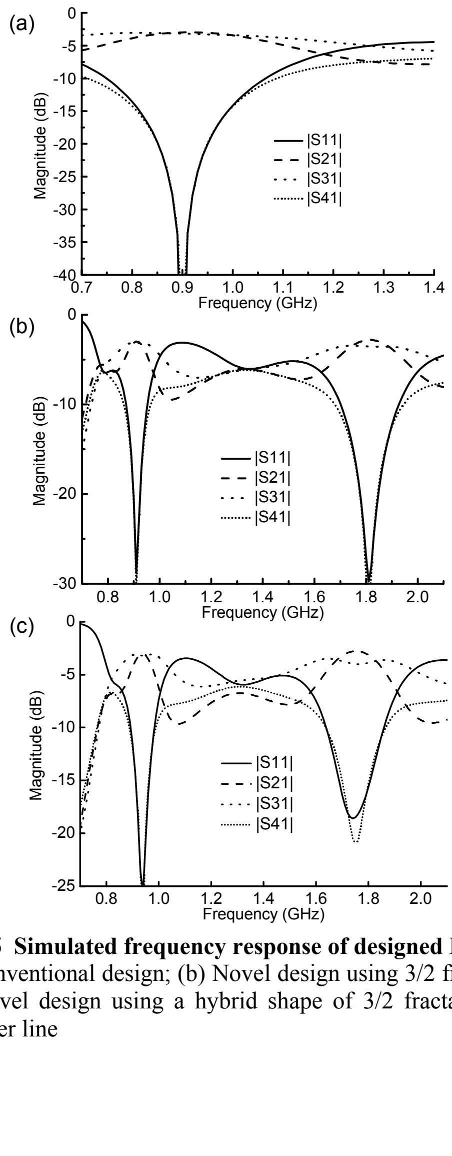

Fig. 5 Simulated frequency response of designed BLCs
(a) Conventional design; (b) Novel design using 3/2 fractals; (c) Novel design using a hybrid shape of 3/2 fractals and meander line

3.2 Measured results

To further validate the design concept, a BLC example employing 3/2 fractal curves of the first iteration was fabricated and measured using an Anritsu ME7808A (Anritsu Company, USA) vector network analyzer. Fig. 6 illustrates the fabricated prototype of the proposed BLC. T-networks with chip capacitors and inductors of 0805 packages were cascaded in the fabricated prototype.

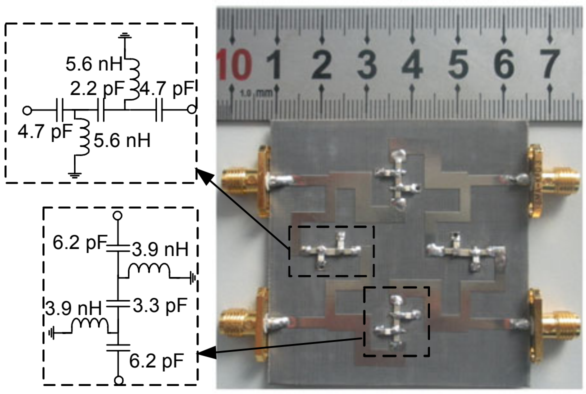

Fig. 6 Fabricated prototype of the proposed dual-band branch-line coupler

Fig. 7a shows the measured frequency response of the fabricated coupler. Experimental results are in good agreement with results from the planar EM simulations except that there was a slightly larger insertion loss together with deteriorative impedance match and isolation in the measured case. The tiny discrepancy between simulation and measurement is introduced mainly through the self-resonance effect of chip components and in part through the tolerance inherent in the fabrication process. Nevertheless, the coupled and transmission insertion losses of the proposed BLC are extremely comparable with regard to other BLCs, e.g., 4.19 and 4.31 dB for the first band and 4.43 and 4.72 dB for the second band of Bonache *et al.* (2008), 4.29 and 4.33 dB, and 3.8 and 4.54 dB for the lower and upper bands respectively, of Chi and Itoh (2009). Consequently, our BLC shows some technical advantages over previous BLCs, e.g., those using complementary split ring resonators (CSRRs) which caused significant radiation loss (Bonache *et al.*, 2008), or adopting three CRLH TL cells which may be directly associated with large insertion losses.

Fig. 7b displays the phase difference between the output ports of the BLC. Almost identical results between simulation and measurement were achieved across the entire frequency range. The phase difference is very accurate, approximately −90° and 90° over the bandwidth of interest around the two operating bands. The excellent phase response of the designed BLC makes the fractal-shaped CRLH TL an attractive technique for use in the design of high precision devices. Table 2 summarizes the detailed measurement performance of the developed coupler.

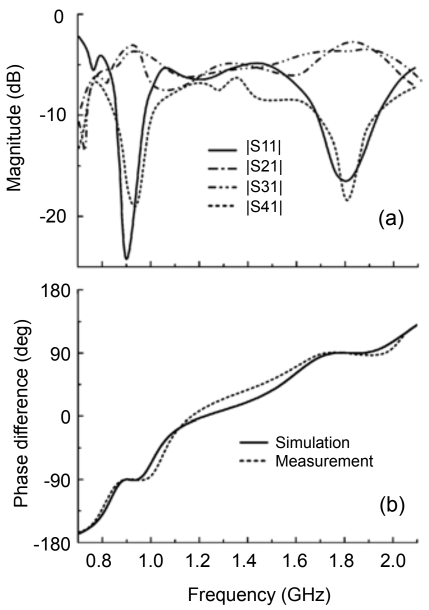

Fig. 7 Measured frequency response (a) and phase difference (∠S21−∠S31) (b) of the novel designed dual-band branch-line coupler

Table 2 Measured results of designed dual-band coupler

Frequency (GHz)	RIL (dB)	IL (dB)	PD (deg)	BW_1 (%)	BW_2 (%)	BW_3 (%)
0.9	24.5, 17.3	3.2, 3.9	90.3	12.4	16.3	9.3
1.8	16.6, 18.5	2.9, 3.96	89.6	13.4	18.2	10.4

RIL: return and isolation loss |S11| and |S41| at f_0; IL: insertion loss |S21| and |S31| at f_0; PD: phase difference between ports 2 and 3 (∠S21−∠S31). BW_1: relative communal bandwidth of 10 dB return and isolation loss $(f_2-f_1)/f_0$; BW_2: relative bandwidth of amplitude difference (||S21|−|S31||≤1 dB); BW_3: relative bandwidth of phase imbalance (|∠S21−∠S31|−90°|≤1°)

4 Conclusions

A novel fractal-shaped CRLH TL using lumped elements is first exploited in terms of miniaturization and dual-band realization. To illustrate its possible application, two essentially compact DB BLCs operating at 0.9 and 1.8 GHz are proposed and researched. The design concept was verified by simulation and experimentally demonstrated by measurement data. Fractal perturbation appears without any virulent deterioration on the coupler performance, especially in terms of the DB behavior. The effective occupied areas of the fractal-shaped and hybrid fractal-shaped DB BLCs have been significantly reduced, by 49.7% and 64.1%, respectively. To the best of our knowledge, this is one of the simplest and most interesting approaches available for realizing miniaturization. The space-filling property of fractals and the hyperbolic-linear dispersion relation of the CRLH TL make the combined technology an attractive approach for the design of compact DB components.

References

Bahl, I., 2003. Lumped Elements for RF and Microwave Circuits. Artech House, Boston, p.462-465.

Bonache, J., Sisó, G., Gil, M., Iniesta, Á., García-Rincón, J., Martín, F., 2008. Application of composite right/left handed (CRLH) transmission lines based on complementary split ring resonators (CSRRs) to the design of dual-band microwave components. *IEEE Microw. Wirel. Compon. Lett.*, **18**(8):524-526. [doi:10.1109/LMWC.2008.2001011]

Chen, W.L., Wang, G.M., 2008. Design of novel miniaturized fractal-shaped branch-line couplers. *Microw. Opt. Technol. Lett.*, **50**(5):1198-1201. [doi:10.1002/mop.23316]

Chi, P.L., Itoh, T., 2009. Miniaturized dual-band directional couplers using composite right/left-handed transmission structures and their applications in beam pattern diversity systems. *IEEE Trans. Microw. Theory Techn.*, **57**(5):1207-1215. [doi:10.1109/TMTT.2009.2017350]

Ghali, H., Moselhy, T.A., 2004. Miniaturized fractal rat-race, branch-line, and coupled-line hybrids. *IEEE Trans. Microw. Theory Techn.*, **52**(11):2513-2520. [doi:10.1109/TMTT.2004.837154]

Liao, S.S., Peng, J.T., 2006. Compact planar microstrip branch-line couplers using the quasi-lumped elements approach with nonsymmetrical and symmetrical T-shaped structure. *IEEE Trans. Microw. Theory Techn.*, **54**(9):3508-3514. [doi:10.1109/TMTT.2006.880650]

Lin, I.H., de Vincentis, M., Caloz, C., Itoh, T., 2004. Arbitrary dual-band components using composite right/left-handed transmission lines. *IEEE Trans. Microw. Theory Techn.*, **52**(4):1142-1149. [doi:10.1109/TMTT.2004.825747]

Sadat, S., Fardis, M., Dadashzadeh, G., Baee, R.K., 2005. Proximity-Coupled Microstrip Patch Antenna Miniaturization Using New Fractal Geometry. IEEE Antenna and Propagation Society Int. Symp., p.262-266.

Sun, K.O., Ho, S.J., Yen, C.C., van der Weide, D., 2005. A compact branch-line coupler using discontinuous microstrip lines. *IEEE Microw. Wirel. Compon. Lett.*, **15**(8): 519-520. [doi:10.1109/LMWC.2005.852789]

Tang, C.W., Chen, M.G., Tsai, C.H., 2008. Miniaturization of microstrip branch-line coupler with dual transmission lines. *IEEE Microw. Wirel. Compon. Lett.*, **18**(3):185-187. [doi:10.1109/LMWC.2008.916798]

Wang, J.P., Wang, B.Z., Guo, Y.X., Ong, L.C., Xiao, S.Q., 2007. A compact slow-wave microstrip branch-line coupler with high performance. *IEEE Microw. Wirel. Compon. Lett.*, **17**(7):501-503. [doi:10.1109/LMWC.2007.899307]

Xu, H.X., Wang, G.M., Zhang, C.X., 2010a. Fractal-shaped UWB bandpass filter based on composite right/left handed transmission line. *Electron. Lett.*, **46**(4):285-286. [doi:10.1049/el.2010.3139]

Xu, H.X., Wang, G.M., An, H.P., 2010b. Hilbert fractal curves form compact diplexer. *Microw. & RF*, **49**(8):92-95.

Zhang, H.L., Chen, K.J., 2007. A stub tapped branch-line coupler for dual-band operations. *IEEE Microw. Wirel. Compon. Lett.*, **17**(2):106-108. [doi:10.1109/LMWC.2006.890330]

Zhang, Y., Hu, L., He, S.L., 2005. A tunable dual-broad-band branch-line coupler utilizing composite right/left-handed transmission lines. *J. Zhejiang Univ.-Sci.*, **6A**(6):483-486. [doi:10.1631/jzus.2005.A0483]